Ascorbate Peroxidase, a Key Molecule Regulating Amphotericin B Resistance in Clinical Isolates of *Leishmania donovani*

Ashish Kumar,[a] Sushmita Das,[c] Bidyut Purkait,[a] Abul Hasan Sardar,[a] Ayan Kumar Ghosh,[a] Manas Ranjan Dikhit,[b] Kumar Abhishek,[a] Pradeep Das[a]

Department of Molecular Biology[a] and Department of Biomedical Informatics,[b] Rajendra Memorial Research Institute of Medical Sciences, Agamkuan, Patna, Bihar, India; Department of Microbiology, All India Institute of Medical Sciences, Patna, Bihar, India[c]

Amphotericin B (AmB), a polyene macrolide, is now a first-line treatment of visceral leishmaniasis cases refractory to antimonials in India. AmB relapse cases and the emergence of secondary resistance have now been reported. To understand the mechanism of AmB, differentially expressed genes in AmB resistance strains were identified by a DNA microarray and real-time reverse transcriptase PCR (RT-PCR) approach. Of the many genes functionally overexpressed in the presence of AmB, the ascorbate peroxidase gene from a resistant *Leishmania donovani* strain (LdAPx gene) was selected because the gene is present only in *Leishmania*, not in humans. Apoptosis-like cell death after exposure to AmB was investigated in a wild-type (WT) strain in which the LdAPx gene was overexpressed and in AmB-sensitive and -resistant strains. A higher percentage of apoptosis-like cell death after AmB treatment was noticed in the sensitive strain than in both the resistant isolate and the strain sensitive to LdAPx overexpression. This event is preceded by AmB-induced formation of reactive oxygen species and elevation of the cytosolic calcium level. Enhanced cytosolic calcium was found to be responsible for depolarization of the mitochondrial membrane potential and the release of cytochrome *c* (Cyt *c*) into the cytosol. The redox behavior of Cyt *c* showed that it has a role in the regulation of apoptosis-like cell death by activating metacaspase- and caspase-like proteins and causing concomitant nuclear alterations, as determined by terminal deoxynucleotidyltransferase-mediated dUTP-biotin nick end labeling (TUNEL) and DNA fragmentation in the resistant strain. The present study suggests that constitutive overexpression of LdAPx in the *L. donovani* AmB-resistant strain prevents cells from the deleterious effect of oxidative stress, i.e., mitochondrial dysfunction and cellular death induced by AmB.

The parasitic protozoa of the genus *Leishmania* are the causative agents of leishmaniasis and still constitute a major public health problem. It is estimated that globally there are 12 million humans infected with leishmaniasis, with an incidence of 0.5 million visceral-form cases (1). Visceral leishmaniasis (VL) is a systemic protozoan disease that is transmitted by phlebotomine sandflies. Miltefosine, paromomycin, and single-dose liposomal amphotericin B (AmB) are gradually replacing conventional pentavalent antimonials as the preferred treatments (2). Amphotericin B deoxycholate (Fungizone) is the second line of treatment, except in Bihar, India, where it is now the first-line drug because 60% of cases in many areas are resistant to sodium antimony gluconate (SAG) (3).

It has previously been demonstrated that altered membrane composition, ABC transporters, and an upregulated thiol metabolic pathway enzyme have a role in conferring amphotericin B resistance in clinical isolates of *Leishmania donovani* (4). It was also reported that in laboratory-derived AmB-resistant parasites, the major sterol was an ergosterol precursor, cholesta-5,7,24-trien-3-ol, and not ergosterol, which is the key molecule in the AmB-sensitive strain (5).

AmB can affect/kill cells by its auto-oxidation and subsequent formation of free radicals (6). Kinetoplastids, comprising parasites of the genera *Crithidia*, *Trypanosoma*, and *Leishmania*, are devoid of catalase and glutathione (GSH) peroxidase (7, 8), and the removal of hydroperoxides in these parasites presumably relies on the tryparedoxin pathway to regulate oxidative stress (9, 10).

Trypanosoma cruzi expresses an unusual plant-like ascorbate-dependent hemoperoxidase whose activity has been linked to the reduction of the parasite-specific thiol trypanothione by ascorbate in a process that involves nonenzymatic interaction (11). Ascorbate peroxidase (APx) is an integral component of the glutathione-ascorbate cycle. Glutathione, which maintains the reducing milieu of cells, is undoubtedly involved in the reduction of many cellular components (12). It has been reported that the single-copy *Leishmania major* ascorbate peroxidase gene may play an important role in the detoxification of H_2O_2, which is generated by endogenous processes and as a result of external influences, such as the oxidative burst of infected host macrophages or drug metabolism by *Leishmania* (13). The removal of H_2O_2 from amastigotes was markedly inhibited by aminotriazole or sodium azide, an inhibitor of heme-containing enzymes, e.g., catalase and peroxidase (13). *L. major* promastigotes overexpressing ascorbate peroxidase showed enhanced tolerance to apoptosis mediated by oxidative stress. *L. major* APx (LmAPx) overexpressed in the mitochondria of *L. major* protects cells from the deleterious effects of oxidative stress, i.e., mitochondrial dysfunction and cellular death (14).

After exposure to low fungicidal doses of acetic acid, hydrogen

peroxide, and AmB, *Candida albicans* displayed chromatin margination and condensation, nuclear envelope separation, nuclear fragmentation, and DNA damage exposing free 3-OH groups, as determined by the terminal deoxynucleotidyltransferase-mediated dUTP-biotin nick end labeling (TUNEL) assay (15). Cell death induced by low but toxic concentrations of H_2O_2 or amphotericin B triggers the development of a protein synthesis-dependent apoptosis-like phenotype also in the opportunistic pathogen *Aspergillus fumigatus* (16).

In trypanosomatids, many apoptogenic agents or stresses are associated with dysfunction of the unique mitochondrion, as indicated by the changes in mitochondrial membrane potential ($\Delta\Psi$m) (17). A variety of apoptotic stimuli cause cytochrome *c* (Cyt c) release from mitochondria, which in turn induces a series of biochemical reactions that result in caspase activation and subsequent cell death (18). The redox state of Cyt *c* has been shown to be an important factor for Cyt *c*-mediated apoptosis (19). Cytosolic Cyt *c* is oxidized by cytochrome oxidase, and the oxidized Cyt *c* helps the cell to undergo apoptosis by some biochemical mechanism. Several biologically relevant reducing agents, including superoxide (20), ascorbate (21–24), and glutathione (25, 26), are known to reduce Cyt *c*, thus inhibiting Cyt *c*-mediated apoptosis. Therefore, in the cellular redox environment that favors the formation of Fe^{2+}-Cyt *c*, apoptosis can be blocked (27).

AmB chemotherapy has been proven to be very successful in the treatment of VL in the Indian subcontinent, but due to its regular use at high frequency, the emergence of drug-resistant cases is expected. The clinics within Rajendra Memorial Research Institute of Medical Sciences, Patna, Bihar, India, have recorded an incidence of AmB relapse of 1 to 2% of cases (2010 to 2013). Therefore, the major objective of the present paper is to understand the molecular mechanism of AmB resistance in clinical isolates by investigating the involvement of overexpressed *Leishmania donovani* APx (LdAPx) in resistant *Leishmania* parasites and how they are protected against AmB-mediated oxidative stress regulating mitochondrion-mediated apoptosis.

MATERIALS AND METHODS

Collection of clinical isolates. Clinical isolates isolated from splenic aspirates of AmB-responsive and non-AmB-responsive patients were collected from the indoor ward facility of the Rajendra Memorial Research Institute of Medical Sciences, Patna, India, according to our previously published sample collection methodology (4). The study was approved by the Institutional Ethical Committee of the Rajendra Memorial Research Institute of Medical Sciences.

Differential-expression studies. Genes differentially expressed between AmB-resistant and AmB-sensitive parasites were identified using a genomic DNA microarray (GeneTac UC4) technique. Overexpressed genes were further validated by semiquantitative and real-time PCR using SYBR green chemistry (Roche). A shotgun genomic DNA library was constructed from Indian *L. donovani* promastigotes, and the microarray chip was hybridized in an automated hybridization machine (HybStation; Genomic Solutions). Hybridization was performed at 65°C for 3 h, 55°C for 3 h, and 42°C for 12 h (28). The hybridized microarrays were scanned in a UC-4 microarray scanner (Genomic Solutions, USA), and data were quantified and normalized by using QuantArray microarray analysis software (Packard Biosciences, USA). Only spots in which more than 70% of the pixels had a signal above background of at least twice the standard deviation of the local background were considered in subsequent data analysis. The Cy5/Cy3 fluorescence ratios and log-transformed ratios were calculated from the normalized values. Genes whose expression changed 2-fold or more were selected for further analysis. Individual up-

regulated clones were sequenced using an ABI Prism 3130XL genetic analyzer DNA sequencer (Applied Biosystems, USA), and homology was sought with known genes or proteins in the *Leishmania* data bank. The targeted LdAPx gene was further validated by real-time PCR and by semiquantitative PCR. The α-tubulin gene was used as a control for all reactions.

Cloning and antibody production against LdAPx recombinant protein. The LdAPx open reading frame (ORF) was cloned into the Pet28a vector (Calbiochem), and expressed protein was purified by Ni-nitrilotriacetic acid agarose ion-exchange column chromatography according to the manufacturer's protocol (Qiagen). The homogeneity of recombinant protein was checked by SDS-PAGE and used to immunize rabbits for recombinant-LdAPx antibody generation.

***In silico* studies of APx for inhibition.** For homology modeling of *L. donovani* ascorbate peroxidase, restrained base modeling was implemented in the MODELER program (29) using the *L. major* peroxidase crystal structure as the template (Protein Data Bank [PDB] code, 3RIV). The stereo-chemical properties of the models were investigated with a Ramachandran plot using PROCHECK, and the best model was selected. The target model was further refined by loop modeling and side-chain refinement to increase the three-dimensional (3D) score and to make the model reliable. The modeled structure was set for validation by the SAVES (http://nihserver.mbi.ucla.edu/SAVES/) and PROSSA servers. Molecular dynamics assays and simulations were conducted for 4,000 ps (4 ns) of 2,000,000 steps under particle mesh Ewald (PME) electrostatics and NPT (number of particles, system pressure, and temperature) conditions using the GROMACS 4.0.3 (the Groningen Machine for Chemical Simulations) package. To understand the interaction between the *L. donovani* APx binding site and 1H-1,2 4-triazol-5-amine (inhibitor of APx), docking studies were carried out with the DSv2.5 and FLexX docking programs.

Overexpression of LdAPx in sensitive parasites. The LdAPx ORF was PCR amplified for preparation of overexpression constructs using primers with corresponding restriction sites (underlined) (forward, 5′-GGGA<u>AGCTT</u>ATGACAGCGTCTCCGAGAGC-3′; reverse, 5′GGG<u>GGATCCT</u>CACCTCTCATTCGGCGCC-3′) and cloned into the *Leishmania* expression vector pLpneo2 (a kind gift provided by Greg Matlashewski). Cloned pLpneo2 (with the ORF in the right orientation) was transfected into one sensitive laboratory strain (Ag83) by electroporation using a Gene Pulser (Bio-Rad) (13). Parasites transfected with the empty vector, pLpneo2, were taken as controls. Transfectants were selected and maintained in the presence of G418 (40 μg/ml). Overexpression of LdAPx in the sensitive strain was analyzed by Western blotting and reverse transcriptase PCR (RT-PCR) SYBR green chemistry.

Detection of an accumulation of ROS. Reactive oxygen species (ROS) were measured in wild-type AmB-sensitive and -resistant cells as well as in LdAPx-overexpressed AmB-sensitive cells treated with AmB (0.125 μg/ml) by using the H_2O_2-sensitive probe 2′,7′-dichlorohydrofluorescein diacetate (H_2DCFDA) (excitation and emission wavelengths, 488 and 530 nm, respectively). Treated sensitive and resistant parasites (2×10^6 in each set) after 24-h time intervals were incubated with 0.4 mM (final concentration) H_2DCFDA for 15 min in the dark. Cells were then washed twice in phosphate-buffered saline (PBS); subsequently, fluorescence was measured with a BD Aria II fluorescence-activated cell sorter (FACS), and results were analyzed with BD FACS Diva software, version 6.2.1 (BD Bioscience, USA).

Measurement of calcium level. Calcium levels were measured according to the protocol of Ruben et al. (30) using fura-2 acetoxymethyl ester (Fura-2AM) in a PerkinElmer spectrofluorometer at 340-nm excitation and 510-nm emission wavelengths (30). Briefly, 1×10^7 cells/ml of the AmB-resistant strain, AmB-sensitive strain, and both strains treated with aminotriazole were incubated with 0.125 μg/ml AmB and 6.0 μM Fura-2AM for 30 min at 24°C. After incubation, cells were harvested, washed twice with fresh serum-free medium, and analyzed with a fluorescence spectrophotometer.

Analysis of mitochondrial membrane potential. Mitochondrial membrane potential was measured using JC-1 dye (5,59,6,69-tetrachloro-1,19,3,39 tetraethylbenzimid azolylcarbocyanine iodide), a cell-permeable dye that exists in a monomeric form that, on entering the cytoplasm, emits a green fluorescence. Subsequently, upon entering the mitochondria, it forms aggregates and emits a red fluorescence. The ratio between red and green fluorescence, i.e., 585/530 nm, determines the mitochondrial membrane potential (24). After being treated with AmB (0.125 μg/ml) for 24 h, sensitive and resistant cells that had wild-type levels of LdAPx expression, sensitive cells in which LdAPx was overexpressed, and cells in which ascorbate peroxidase expression was inhibited were centrifuged (825 × g for 10 min). The cells were resuspended in PBS containing JC-1 dye (10 mg; Molecular Probes) and incubated at 24°C for 15 min. Analysis for mean green and red fluorescence intensities was done using a BD Aria II FACS and BD FACSDiva software.

Detection of Cyt *c* released by mitochondria. Release of cytochrome *c* from mitochondria into the cytoplasm after AmB treatment in both the resistant and the sensitive strain was evaluated by Western immunoblotting using a BD ApoAlert cell fractionation kit by following the manufacturer's instructions (Clontech, Palo Alto, CA, USA) (31). Briefly, resistant cells incubated with AmB, with and without the inhibitor (aminotriazole), were harvested, washed twice with PBS, suspended in cell fractionation buffer, and homogenized. Cytosolic and mitochondrial fractions were fractionated by differential centrifugation. Proteins samples (50 μg) from cytosolic fractions were separated by 12% SDS-PAGE and Western immunoblotted with rabbit polyclonal anti-cytochrome *c* antibody. Reactive bands were detected by using 5-bromo-4-chloro-3-indolylphosphate (BCIP) and 4-nitroblue tetrazolium chloride (NBT).

Reduction of Cyt *c*. Cytochrome *c* (Cyt *c*) is well known for its role in mitochondrial electron transport. The redox state of Cyt *c* has recently been linked to apoptosis. Various biological reductants, including superoxide, ascorbate, glutathione (GSH), and cysteine, and some reducing enzymes (e.g., nitric oxide synthase) have been demonstrated to reduce Cyt *c*, thus inhibiting Cyt *c*-mediated apoptosis. The reaction was studied by mixing the proper quantities of solutions of cytochrome *c* with thiol-ascorbate at physiologically relevant concentrations. The final concentrations of Cyt *c*, thiols, and ascorbate in the reaction mixture were 5 μM, 100 μM, and 50 μM, respectively. All kinetic measurements were taken by monitoring the changes in absorbance at 550 nm for 5 min at 25°C with a spectrophotometer. All solutions were buffered at pH 7.4 with 50 mM Tris HCl.

Effect of redox behavior of Cyt *c* on caspase-like protease activity. For evaluation of Cyt *c*-induced caspase-like protein activation *in vitro*, cell homogenates were supplemented with 100 nM Cyt *c* plus 1 mM ATP and incubated for 20 min with 100 μM Asp-Glu-Val-Asp–7-amino-4-trifluoromethyl coumarin [DEVD-AFC]). Redox-active agents (10 mM ascorbate, 120 mM cytochrome *c* oxidase) were used; cytochrome *c* was preincubated with them for 5 min and then added to the cytosols. The level of free AFC was determined fluorimetrically at a maximum wavelength of 521 nm by spectrofluorimetry (PerkinElmer). The developed fluorochrome was proportional to the concentration of caspase-like activated protein.

Detection of caspase 3 and metacaspase-like protease activity. To check whether released cytochrome *c* activates caspase-like protease in *L. donovani*, we measured caspase 3- and metacaspase-like protease activities after treatment with AmB for 24 h. Cell lysates were incubated with corresponding caspase buffers to detect the CED3/CPP32 group of protease activities. Fluorogenic peptide substrates, namely, DEVD-AFC at 100 μM (Optimum) and 1× reaction buffer containing 100 mM dithiothreitol (DTT), were added to corresponding cell lysates to measure the activities of the CED3/CPP32 group of proteases. In a parallel set of reactions, 1 μl of the CED3/CPP32 group of protease inhibitors (*N*-benzyloxycarbonyl-Val-Ala-Asp [OMe]-fluoromethyl ketone [Z-VAD-FMK]) was added to the reaction mixture before the addition of cell lysates. AFC release was

measured with the help of a PerkinElmer LS-55 spectrometer (PerkinElmer) at excitations of 390 to 400 nm and emissions of 510 to 550 nm.

Metacaspase-like protease activity was measured fluorimetrically using the butyloxycarbonyl (Boc)-GRR-amino methyl coumarin (AMC) substrate as described by Lee et al. (32), with minor modifications. Briefly, promastigote cultures were pelleted by centrifugation and resuspended in fresh culture medium containing 0.12 μg/ml AmB, and sample was incubated for 24 h at 26°C. Antipain (a metacaspase inhibitor) at 1.0 μM was added to control reaction mixtures for 30 min before the addition of AmB. Treated or untreated parasites were lysed (10^8 cells/ml) in lysis buffer (50 mM Tris-HCl, pH 7.5, 1% [vol/vol] Triton X-100, 10% [wt/vol] sucrose, 150 mM NaCl) for 30 min on ice, and the insoluble material was eliminated by centrifugation at 15,000 × g for 20 min at 4°C. One hundred fifty microliters of the supernatant was incubated with a fluorogenic substrate (Boc-GRR-AMC; 75 μM), 5 mM DTT, and 10 mM $CaCl_2$ for 2 h at 37°C under gentle agitation and transferred to a microwell plate. The sample was analyzed immediately with a fluorescence spectrophotometer at an excitation of 355 nm and an emission of 460 nm. Protease activity was expressed in relative fluorescence units.

Apoptosis assessment by the TUNEL assay and flow cytometry. Flow cytometry forward and side scattering was used for gating the *Leishmania* population; 10^4 events were counted per sample. Data were acquired from individual gated populations in a FACS, and results were analyzed with BD FACS Diva software, version 6.2.1 (BD Bioscience, USA). FL1 log data (*x* axis) versus the FL2 log data (*y* axis) were acquired. The irrelevant isotype control was used to define nonspecific staining, which was adjusted to less than 1% of apoptotic cells. The mean fluorescence intensity (MFI) was estimated from the obtained data. TUNEL staining was performed with an *in situ* cell death detection fluorescein kit (Roche, Germany) to detect *in situ* DNA fragmentation according to the manufacturer's manual. Briefly, AmB-treated sensitive and resistant cells and sensitive cells in which LdAPx was overexpressed (1 × 10^6 cells) were harvested and washed twice with 1× PBS. Fixation solution (100 μl) was added, and the cells were resuspended and incubated at 15°C to 25°C in a shaker for 1 h. Cells were centrifuged, PBS was removed, and cells were resuspended in permeabilizing solution for 2 min on ice. Cells were washed again in PBS, and the pellet was resuspended in the TUNEL reaction mixture (50 μl/ml). The plate was incubated for 1 h at 23°C under humidified conditions in the dark. Cells were washed and resuspended to a final volume of 250 μl in 1× PBS and directly analyzed in the FACS.

Detection of DNA fragmentation. Total genomic DNA was isolated using an apoptotic DNA laddering kit (Roche) from both sensitive and resistant strains before AmB treatment; afterwards, sensitive and resistant cells and sensitive cells in which LdAPx was overexpressed were treated with AmB for 24 h, and the sensitive strains were preincubated with the broad-spectrum caspase inhibitor Z-VAD-FMK. Cells were pipetted out from the wells in 1.5-ml Eppendorf tubes, and the DNA laddering assay was performed according to the manufacturer's protocol. Precisely, 2 × 10^6 cells were pelleted down by centrifugation at 2,000 × g for 10 min, and finally a 200-μl sample with 1× PBS was prepared. Binding buffer/lysis buffer (200 μl) was added, and samples were incubated for 10 min at 15 to 25°C. One hundred microliters of isopropanol was added, and then the sample was shaken and pipetted out to the upper reservoir of a filtration apparatus. Finally, after three washes, 200 μl of prewarmed (70°C) elution buffer was added. Electrophoresis of the isolated DNA was performed in 1% agarose gel.

Inhibitor assay. Aminotriazole, an ascorbate peroxidase inhibitor, was added at a 5 μM final (optimal) concentration to sensitive and resistant cells and sensitive cells in which LdAPx was overexpressed and incubated for 2 h at 23°C in a biochemical oxygen demand (BOD) incubator prior to AmB treatment to study aminotriazole's effect on the change from AmB resistance to AmB sensitivity. The parasites were subsequently washed with PBS (pH 7.2) and treated with AmB (0.125 μg/ml).

Statistical analysis. The data were statistically analyzed by the Student *t* test and are presented as means and standard deviations of three deter-
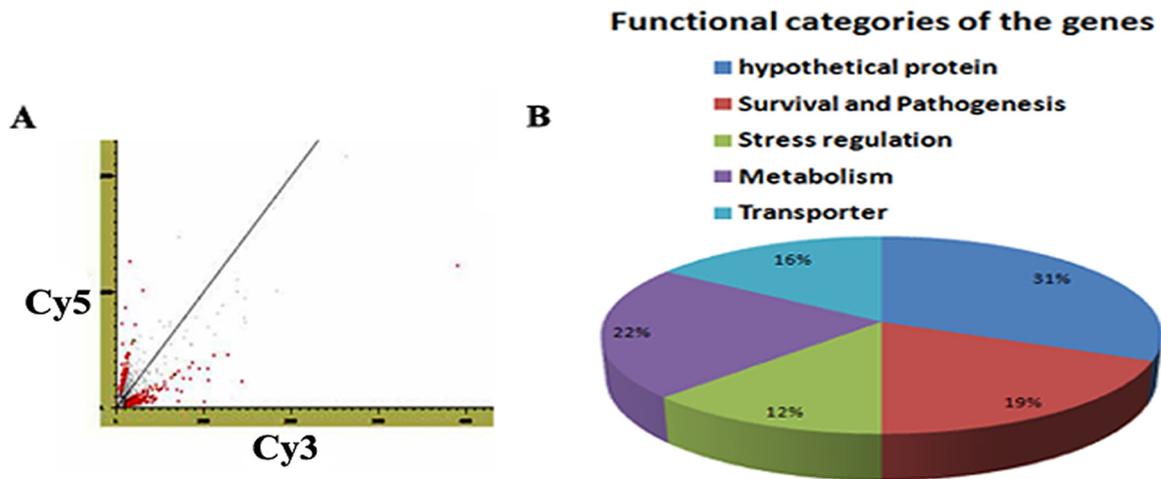
FIG 1 Differential gene expression between AmB-sensitive and -resistant parasites. (A) Scatter plot showing the distribution of signal intensities generated by DNA microarray. (B) Distribution of differentially expressed genes on the basis of their functional characterizations.

minations from at least two independent experiments. A *P* value of <0.05 was considered significant.

Nucleotide sequence accession number. The complete sequence of the LdAPx gene was submitted to the NCBI GenBank database under accession no. JN802370.

RESULTS

Characterization of clinical isolates. In our previous study (4), we characterized in greater detail the AmB-resistant and -sensitive nature of clinical isolates by both *in vitro* and *ex vivo* drug sensitivity assays, and the 50% lethal dose (LD_{50}) for the resistant strain was found to be 8-fold higher than that for the sensitive strain. These strains were maintained in our laboratory, and the same were used in the present study.
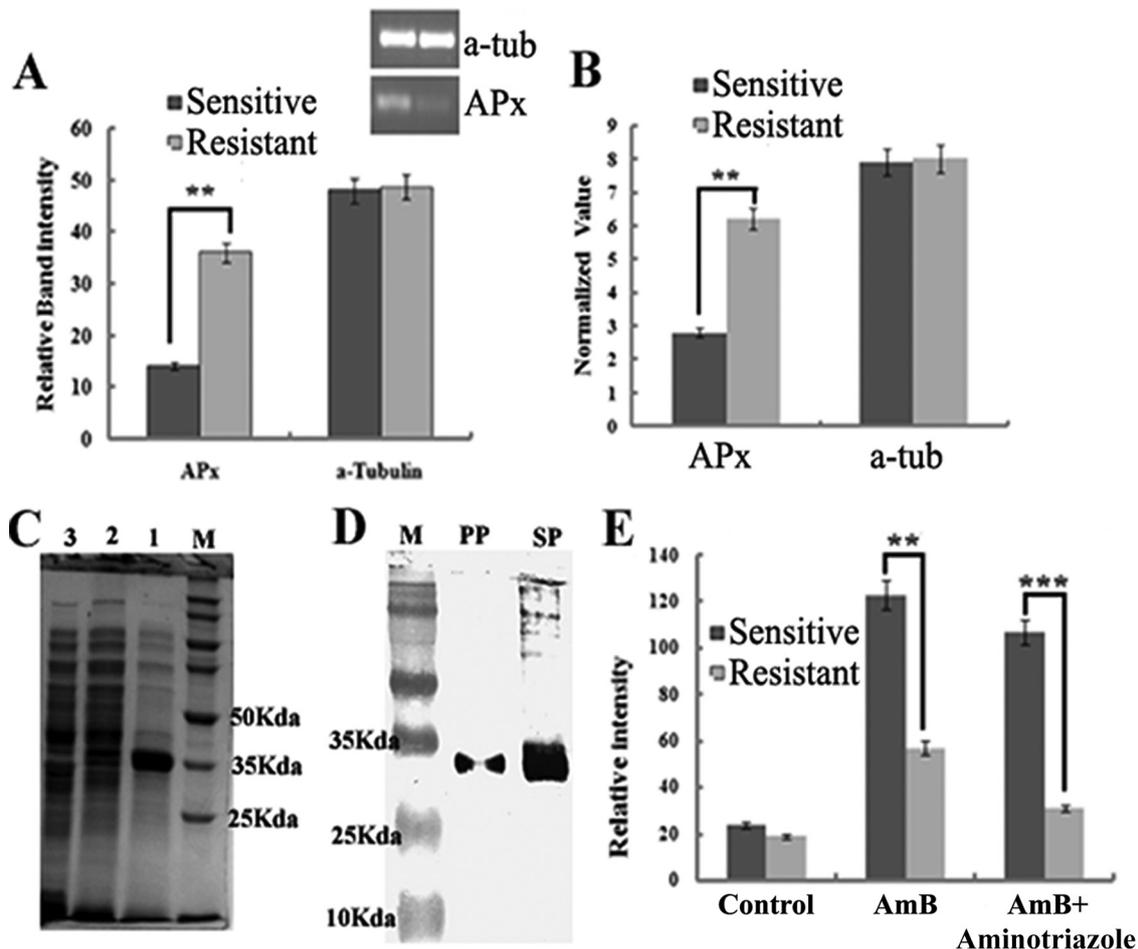
Overexpression of LdAPx in the resistant strain. Microarray analysis revealed that many genes were found to be differentially expressed (~3-fold upregulation) ($P < 0.005$) in the resistant strain (Fig. 1A) compared to sensitive ones. On the basis of their predicted functionality, analysis shows that 31% of the genes are hypothetical genes, 22% are metabolic genes, 19% are genes that help in survival and pathogenesis, 16% are transporter genes, and 12% help in stress regulation (Fig. 1B). The upregulated LdAPx gene was selected due to its overexpression, which suggested that it may have some role in resistance and because it is present only in parasites, not in humans. Microarray data for LdAPx were further analyzed by semiquantitative (Fig. 2A) and real-time (Fig. 2B) PCR. At the mRNA level, the LdAPx gene was found to be ~2.9- and ~3.2-fold upregulated in the resistant strain compared to the sensitive strain.

Immunoblot analysis. Using the *Leishmania infantum* genome project (NCBI, GenBank), the sequence corresponding to the open reading frame (ORF) of ascorbate peroxidase was retrieved (XM_001468357.1). The coding sequence for the protein was amplified from genomic DNA of *L. donovani* by PCR, producing a single amplicon of 912 bp (data not shown). After the cloning, expression, and purification, the LdAPx fusion protein exhibited a 35-kDa size (Fig. 2C). The purified protein was blotted against monoclonal anti-His antibody and showed a single band (Fig. 2D). The activity of the LdAPx recombinant protein was checked by time dependence inactivation of APx by H_2O_2 and

aminothiazole inhibition assays. These inhibition profile data strongly suggest the authenticity of the APx protein (Fig. 1 and 2; see also the supplemental material). Antibody generated against that purified protein showed a high titer.

Structure of LdAPx. The template search was based on sequence identity and was carried out using BLASTP against sequences in the PDB. The crystal structure of *Leishmania major* peroxidase (PDB code 3RIV_A) at a 1.76-Å resolution was observed as the best template, with 96% sequence identity and 97% positive hits. Ten different models of LdAPx were built using MODELLER 9v2 (33). Based on the Ramachandran plot and on the discrete optimized protein energy (DOPE) score, a model was designed and used for the rest of the study (Fig. 3A). The final structure with lowest energy was checked by Profile-3D (DS 2.5); the self-compatibility score for this protein is 112.7, which is much higher than the lowest score (62.04) and close to the top score (137.88). The target model was further refined by loop refinement tools of DS2.5, and the self-compatibility score increased to 123.71, which is very close to a high-verification score (137.88). ProSA-web analysis showed local model quality by plotting energies as a function of amino acid sequence position. The plot shows that the energy remains negative for almost all amino acid residues, indicating the acceptability of the predicted model (Fig. 3B). The overall geometric environment profile calculation of the model determined by the ERRAT program was 87.11%. Molecular dynamics (MD) simulations were conducted for modeled systems in explicit solvent using the GROMACS 4.0.3 (The Groningen Machine for Chemical Simulations) package (Fig. 3C). Aminotriazole, an inhibitor of APx (DS2.5 and FLexX software), showed that the Glu133, Val127, and Ser301 amino acids may play a key role in the inhibition of *L. donovani* APx (Fig. 3D).

Overexpression of LdAPx in sensitive *Leishmania* parasites. To see whether overexpression of LdAPx would modulate the AmB sensitivity of parasites, the gene was overexpressed in the sensitive *L. donovani* strain Ag83. The presence of the LdAPx gene in transfectants was confirmed by Western blotting and RT-PCR. The upregulation of LdAPx in the sensitive strain was verified at the protein level by Western blotting with anti-LdAPx antibodies. LdAPx was upregulated (~1.5-fold) in sensitive pLpNeo2-LdAPx
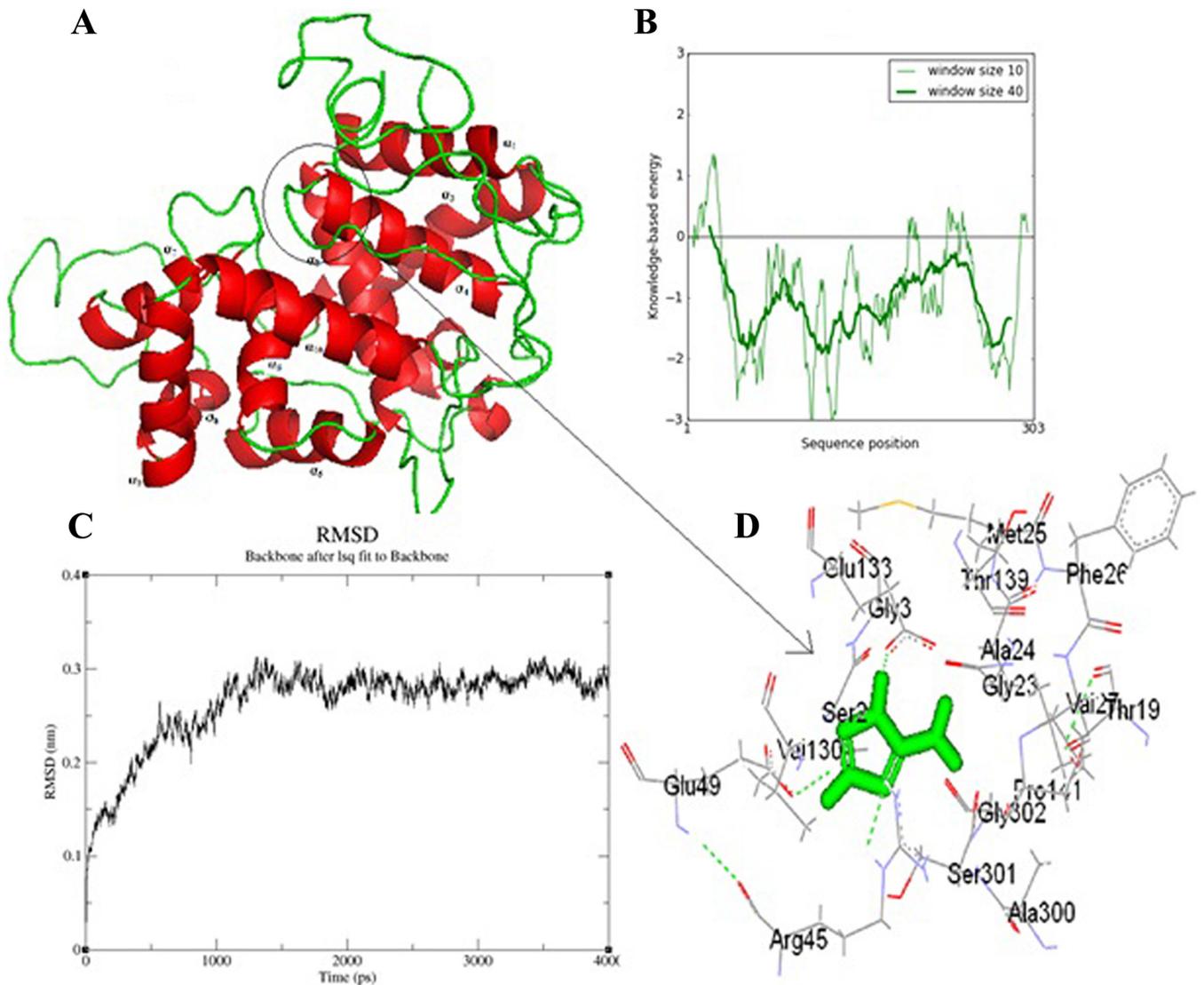
FIG 2 (A and B) Overexpression of LdAPx in a microarray was validated by semiquantitative RT-PCR and real-time PCR. a-tub, α-tubulin. (C) Expression of the recombinant protein. Lane M, molecular mass markers; lane 1, total cellular protein after isopropyl-β-D-thiogalactopyranoside (IPTG) induction; lane 2, cells carrying the vector with the insert before IPTG induction; lane 3, cells carrying the vector without the insert. (D) Western blot analysis using anti-His monoclonal antibody. Lane M, molecular mass markers; PP, gel-eluted purified recombinant protein; SP (supernatant protein), total cellular protein after IPTG induction. (E) Release of cytosolic calcium ions after treatment with AmB in sensitive and resistant strains and strains preincubated with an LdAPx inhibitor (aminotriazole).**, significant difference ($P < 0.005$); ***, significant difference ($P < 0.002$).

parasites compared to its level in sensitive wild-type parasites (Fig. 4A). The overexpression of LdAPx in the sensitive strain was also verified by semiquantitative RT-PCR. Figure 4B depicts a very intense band in the sensitive-strain parasites transfected with the pLpNeo2-LdAPx construct compared to the band intensity of the sensitive wild-type strain, suggesting that the LdAPx transcript was present in the transfectants at high copy numbers. The band intensities of the LdAPx amplicon were 1.8- and 2.96-fold higher (calculated by densitometric analysis using Gel-Doc software) in the sensitive wild type and the sensitive pLpNeo-APx transfectant strain, respectively, than in the resistant strain. The overexpression of LdAPx in the wrong orientation and transfection with the empty vector did not have any effect on parasite sensitivity to AmB (data not shown). Overexpressed LdAPx-sensitive transfectants were maintained at 40 μg/ml G418.

Overexpression of LdAPx confers an increase in tolerance to AmB-mediated ROS. To evaluate the consumption of ROS in AmB-sensitive and -resistant isolates and in the sensitive isolate in which LdAPx is overexpressed, inhibition of the ascorbate peroxidase gene in all strains was measured to determine intracellular

levels of ROS by using the fluorescent probe DCFDA. In our previous study (4), we have shown that the ROS level in the sensitive strain was ~4-fold higher than that of the resistant strain at 24 h of incubation with the drug. Treatment with the ascorbate peroxidase inhibitor significantly increased the level of ROS in the resistant strain compared to that in the resistant wild type ($P < 0.001$); however, the ROS level was not significantly different in sensitive parasites ($P < 0.08$). The LdAPx-overexpressing cell line showed an approximately 1.5-fold decrease in ROS compared with the ROS level in the sensitive wild-type strain ($P < 0.0001$), indicating that LdAPx might have a role in the detoxification of endogenous ROS (Fig. 5).

LdAPx overexpression prevents AmB-mediated-oxidative-stress-induced elevation of cytosolic calcium in the resistant strain. Mitochondrial dysfunction may result in a change in cation homeostasis brought about by high ROS levels. Mukherjee et al. (34) have shown that oxidative stress causes mitochondrial depolarization in *L. donovani* by increasing cytosolic Ca^{2+} levels. Sen et al. (35, 36) showed that calcium flux is necessary not only for the activation of different proteases but also for the appearance

FIG 3 (A) Based on the DOPE score and Ramachandran plot analysis, a reliable model was predicted. The model is based on the published crystal structure for the *L. major* ascorbate complex. (B) The final structure with the lowest energy was checked by Profile-3D (DS 2.5). The plot shows the energy level of the predicated model, which remains negative for almost all amino acids. (C) An MD simulation was conducted for the modeled system in explicit solvent using GROMACS 4.0.3. The root mean square difference (RMSD) in C-α backbone atom in LdAPx for up to 4 ns after the 12-ps model attains its maximum stability is shown. lsq, least-squares. (D) Docking study of aminotriazole (inhibitor of peroxidase enzymes) with the ascorbate peroxidase protein. The result obtained from DS2.5 and FLexX suggest that the Glu133, Val 127, and Ser 301 amino acids may play a key role in the inhibition of *L. donovani* APx.

of phosphatidylserine on the outer leaflet of the plasma membrane during apoptosis. Considering the importance of cytosolic Ca^{2+} in the induction of apoptosis, we measured the Ca^{2+} concentration in the sensitive and resistant strains after AmB treatment and observed that the cytosolic Ca^{2+} level was 2.04-fold higher in the sensitive strain than in the resistant strain ($P <$ 0.005) (Fig. 2 E). After inhibition of the ascorbate peroxidase gene by aminotriazole in the AmB-treated sensitive and resistant strains, we observed that the released cytosolic Ca^{2+} was ~1.8-fold lower in the inhibited resistant strain than in the resistant wild-type strain, while there was no significant change observed with the sensitive strain.

LdAPx overexpression prevents amphotericin B-mediated changes in mitochondrial potential. The loss of mitochondrial membrane potential is a characteristic feature of metazoan apop-

tosis and has been observed to play a key role in drug-induced death in protozoans such as *Leishmania* (26, 27). Flow cytometric analysis showed that after exposure for 24 h to 0.125 μg/ml AmB, the loss in mitochondrial membrane potential, demonstrated by the intense green fluorescence in the cytoplasm, was greater in the sensitive than in the resistant strain. The strain in which LdAPx was overexpressed had reduced apoptosis-like cell death compared to that of the sensitive wild-type strain ($P < 0.001$). The cells in the AmB-treated sensitive and resistant strains were 68.4% (Fig. 6A) and 13.7% (Fig. 6B) apoptotic, respectively, while aminotriazole-treated cells showed 65.3% (Fig. 5A) and 41.3% (Fig. 6B) apoptosis-like death. The mean fluorescence intensity was 5.44-fold higher in the sensitive strain than in the resistant strain ($P <$ 0.005), but after use of the peroxide inhibitor (aminotriazole) in both strains, the percentage of cells exhibiting apoptotic death in
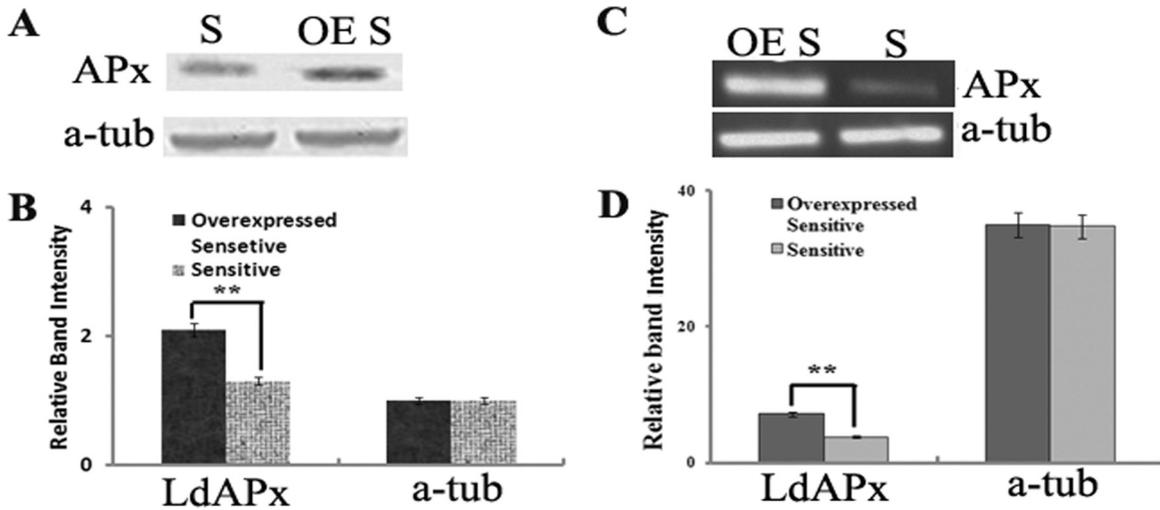
FIG 4 (A) Verification of the LdAPx expression patterns of the AmB-sensitive isolate (S) and of the sensitive isolate in which LdAPx is overexpressed (OE S) by Western blot analysis using anti LdAPx antibody. (B) Densitometric analysis of blotted protein using gel-Doc software. (C) RT-PCR analysis shows the overexpression of LdAPx in the sensitive strain compared to its level in the sensitive wild-type strain. (D) Relative band intensities of the expression level of APx in the sensitive strain in which LdAPx is overexpressed and in the sensitive wild-type strain.

the resistant strain was 3.25-fold higher than in the cells treated only with AmB ($P < 0.002$), while there was no significant difference found in the sensitive strain (Fig. 6A and B).

Release of cytochrome *c* after AmB treatment. Cytochrome *c* is released into the cytoplasm after disruption of the outer mitochondrial membrane by apoptotic stimuli and is an important feature of metazoan apoptosis. Release of Cyt *c* was measured in cytoplasmic protein fractions (50 μg each) of sensitive and resistant strains after treatment with AmB and AmB plus aminotriazol for 24 h through Western blot using anti-cytochrome *c* antibody.

Densitometry analysis of the Western immunoblot showed that at 24 h, cytoplasmic Cyt *c* was 2.8-fold higher in the sensitive strain than in the resistant strain in AmB-treated cells (Fig. 7, top left, lanes a). Moreover, the aminotriazole-preincubated cells in AmB-treated/untreated sensitive and resistant strains showed a higher release of cytochrome *c* in the resistant strain than in the untreated resistant strain (Fig. 7, top left, lane b). From the above data, it may be concluded that (i) in the resistant strain, overexpressed LdAPx reduces the ROS-induced loss in mitochondrial membrane potential that leads to a release of cytochrome *c* from the mitochon-
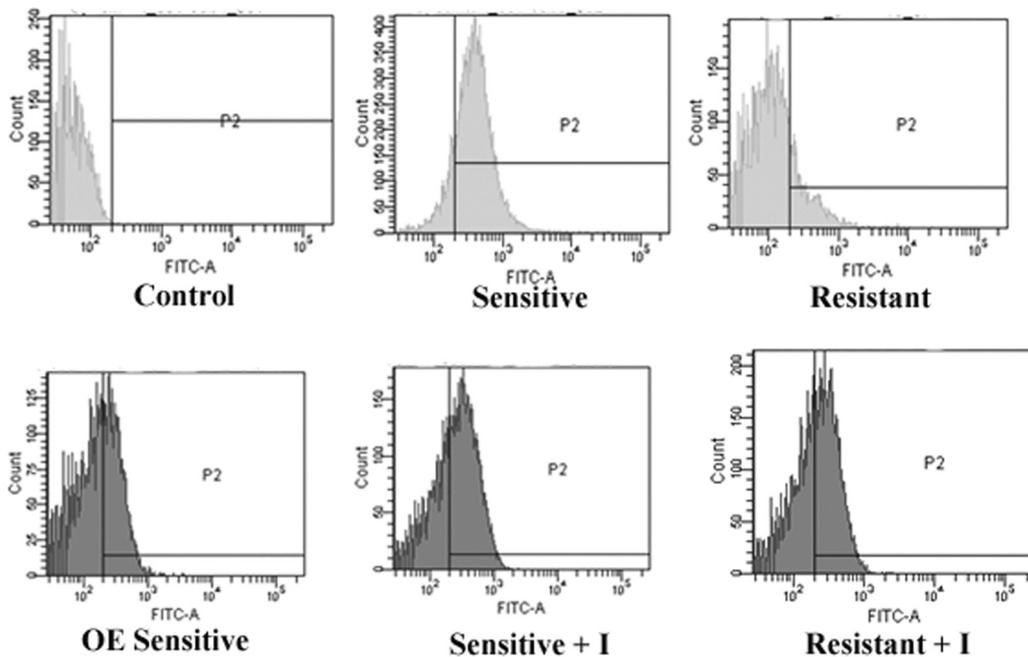

FIG 5 Comparative study of ROS with the fluorescent probe DCFDA after AmB incubation of the sensitive strain, the resistant strain, the sensitive strain in which LdAPx is overexpressed, and both the sensitive wild-type and resistant strains preincubated with ascorbate peroxidase (+ I). FITC-A, fluorescein isothiocyanate area.
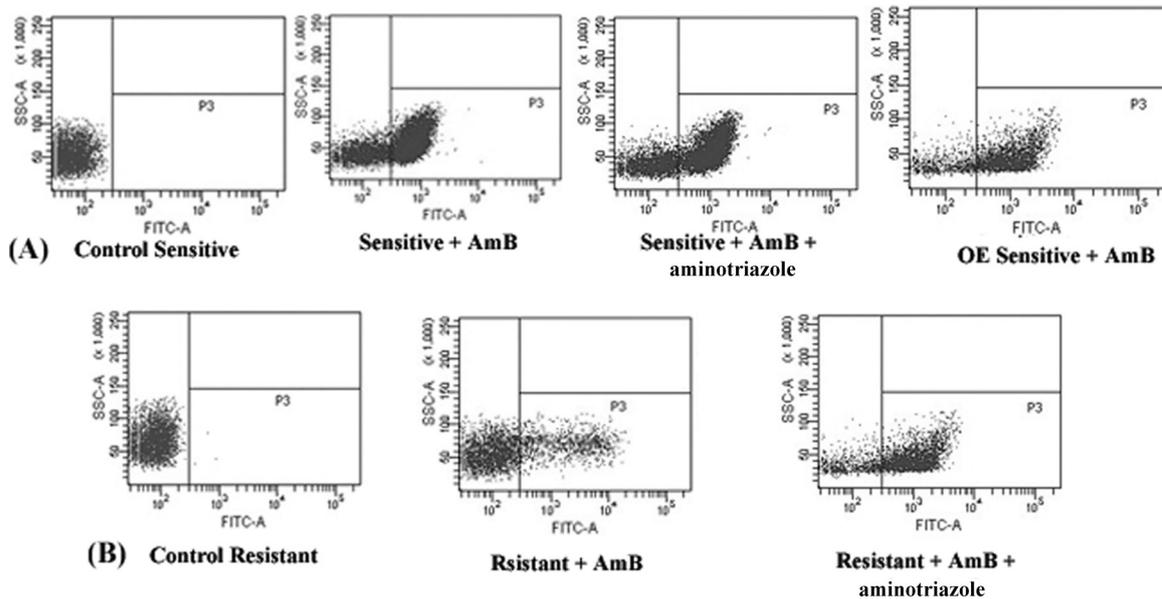
FIG 6 (A and B) Determination of mitochondrial potential in sensitive and resistant parasites through flow cytometric analysis. Cells of the sensitive wild-type strain, sensitive LdAPx overexpression strain (OE), resistant strain, and sensitive and resistant strains preincubated with both aminotriazole and AmB were treated with AmB. The cells in the bottom right quadrant indicate apoptosis. SSC-A, side scatter area.

dria into the cytoplasm but that (ii) after inhibition of ascorbate peroxidase by aminotriazole, the amount of cytoplasmic cytochrome *c* released increases. The results prove that mitochondrial ROS is responsible for the release of cytochrome *c* from mitochondria to the cytosol.

Overexpressed LdAPx-mediated reduction of Cyt *c*. Cyt *c* is a positively charged protein at neutral pH, with theoretical net charges of +9 and +8 for oxidized and reduced Cyt *c*, respectively (24). The reduction of Cyt *c* is a process in which the redox center, heme iron (Fe^{3+}), receives an electron from an electron donor. In the present study, we investigated and compared the kinetics of Cyt *c* reduction by various overexpressed thiol antioxidants as well as ascorbate. The measurement of the cytosolic extract at 550 nm for 5 min demonstrates an increase in the reduced activity of Cyt *c* by ascorbate and glutathione in AmB-treated cells; in untreated cells, Cyt *c* initially increases and then maintains a constant level (Fig. 7, top right).

The redox behavior of cytochrome *c* regulates caspase activity. After the addition of preoxidized cytochrome *c*, caspase-like protease activity was found to be higher (0.96) in the sensitive strain than in the resistant strain (0.55). Likewise, with reduced (with ascorbate) cytochrome *c*, caspase-like protease activity was reduced to a much lower level in the resistant strain (0.27) than in the sensitive strain (0.64), whereas in the presence of Cyt *c*, the control strain was not significantly different from both the resistant and sensitive strains. These observations indicate that the redox behavior of cytochrome *c* regulates caspase-like protease activity (37) (Fig. 7, bottom right).

AmB causes the activation of caspase- and metacaspase-like protease activity in the cytosol. The release of cytochrome *c* from the mitochondria into the cytosol leads to an activation of the caspase-like protein (38), and this is a critical step in the activation of caspase-like protein, which triggers the downstream events leading to apoptosis (39). To further substantiate the existence of these proteases in AmB-sensitive and -resistant clinical isolates of

L. donovani, we carried out a fluorometric assay of CED3/CPP32 family proteases using their specific substrates, DEVD and AFC. The activities were measured in terms of liberation of AFC from their substrates. AmB-treated sensitive strains showed ~3-fold higher caspase 3-like activity than the resistant strain. This increased activity was inhibited by the caspase inhibitor Z-VAD-FMK (Fig. 7, bottom left).

In order to compare the levels of *L. donovani* metacaspase activity in the AmB-treated sensitive and resistant parasites, enzyme assays were done with lysates of both strains and cells were harvested at mid-log growth and reacted with Boc-GKR-AMC as the substrate. Results showed that the sensitive-strain cell lysates contained approximately 3-fold-higher GKRase enzyme activity than lysates of the resistant strain (data not shown). When the metacaspase activities of these strains were compared with those of sensitive LdAPx overexpression and sensitive wild-type strains, we observed that the metacaspase activity was reduced to ~2-fold in the sensitive LdAPx-overexpressed strain. These data confirmed a role for metacaspase in AmB-induced programmed cell death in *Leishmania*.

TUNEL assay. Terminal deoxynucleotidyltransferase-mediated dUTP-biotin nick end labeling (TUNEL) is a method for detecting DNA fragmentation by labeling the terminal ends of nucleic acids that result from apoptotic signaling cascades. FACS analysis showed that after 24 h of incubation with AmB in the sensitive strain, 81.40% of cells were labeled with terminal deoxynucleotidyltransferase (Fig. 8) but that only 48.01% of the resistant parasites were labeled (*P* < 0.005) (Fig. 8). These observations suggested that cells undergoing apoptosis were preferentially labeled by the TUNEL reaction, and it is 6.89-fold higher in sensitive parasites than in resistant parasites. Overexpressed LdAPx in the sensitive strain reduces the nicking of DNA from that in the sensitive wild-type strain (*P* < 0.02).

AmB induces DNA fragmentation in promastigotes. In mammalian cells, internucleosomal DNA fragmentation is one of
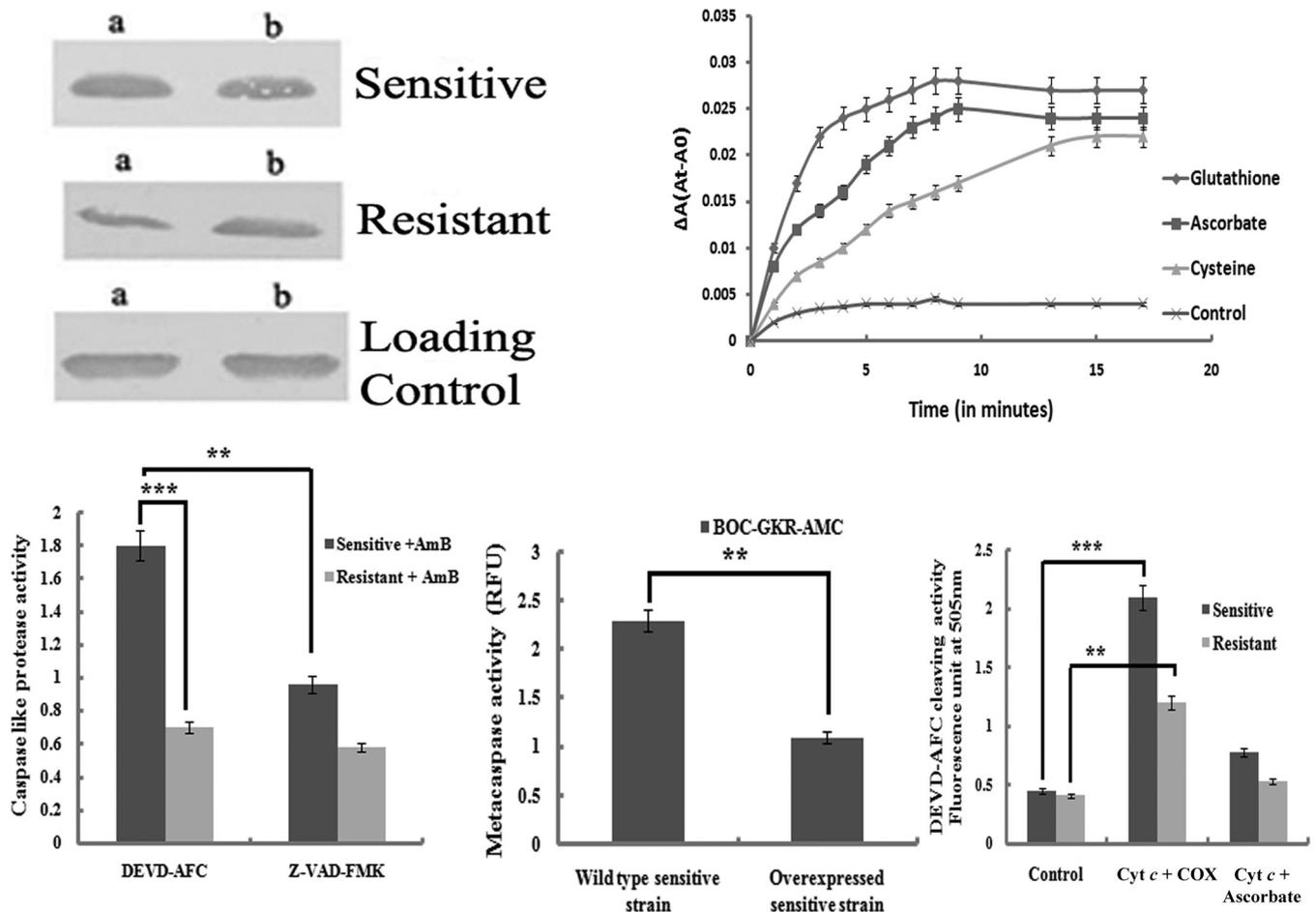
FIG 7 (Top left) Western blot analysis to detect the release of cytochrome *c* into the cytoplasm of differentially treated cells of AmB-sensitive and -resistant strains. Lanes a, cells treated with AmB (0.125 μg/ml) for 24 h; lanes b, cells preincubated with aminotriazole and then AmB for 24 h. (Top right) Kinetic profiles of Cyt *c* reduction by various thiols and ascorbate. ΔA(At-A0), change in absorbance at the indicated time minus the absorbance at time zero. (Bottom left) Comparative study of AmB-induced activation of caspase 3-like protease in sensitive and resistant promastigotes and its downstream effects in the presence of the caspase 3 inhibitor. (Bottom center) Metacaspase activities in the sensitive wild type and in the sensitive strain in which LdAPx was overexpressed. (Bottom right) Oxidized cytochrome *c* (COX) rapidly activated caspase 3 in a cytosolic fraction of the sensitive strain, unlike in the resistant strain, whereas cytochrome *c* reduced by ascorbate or cysteine or glutathione was completely ineffective at activating the caspases in the case of the resistant strain. **, significant difference ($P < 0.05$); ***, significant difference ($P < 0.005$).
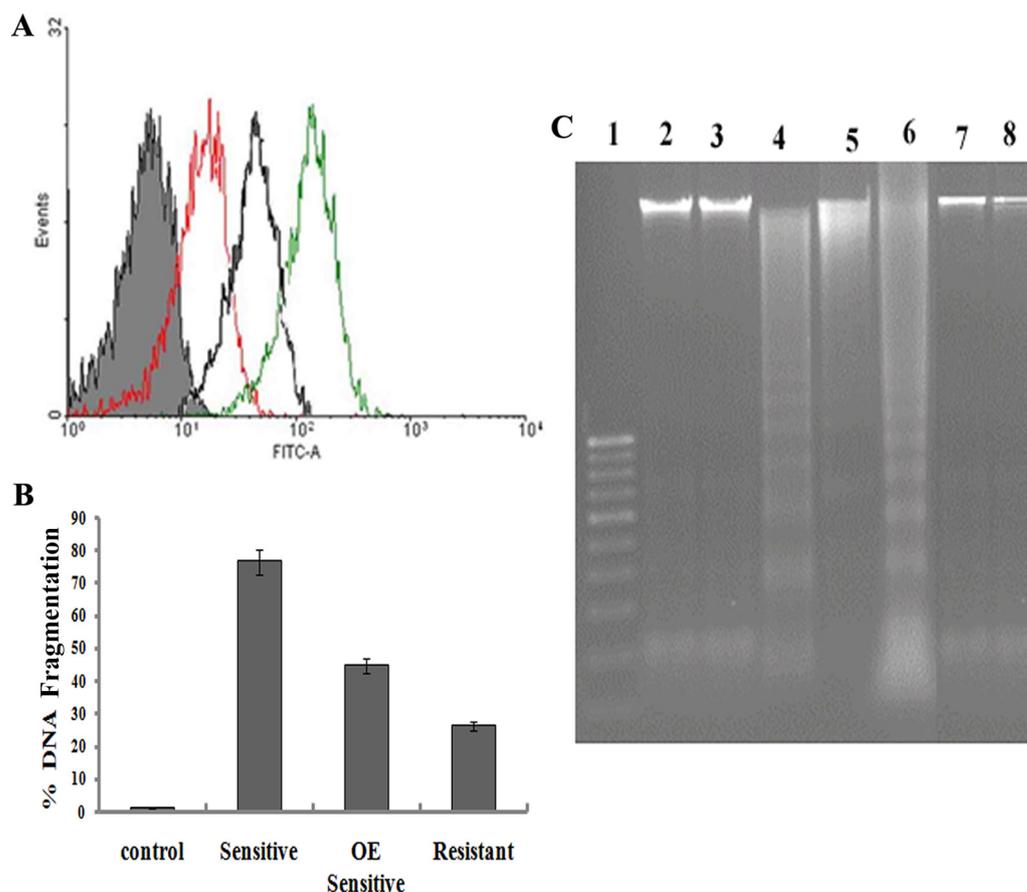
the typical nuclear features of apoptosis (40). DNA analysis by agarose gel electrophoresis revealed a clear DNA fragmentation into oligonucleosome-sized fragments (in multiples of 180 to 200 bp) in sensitive promastigotes treated with 0.12 μg/ml AmB for 24 h (Fig. 8, lane 4), whereas resistant AmB-treated and untreated cells did not show any DNA fragmentation (Fig. 8, lanes 7 and 8). In the presence of a caspase inhibitor (Z-VAD-FMK), DNA fragmentation was prevented in the sensitive strain, while no significant change was observed in the resistant strain (Fig. 8, lanes 2 and 3). The sensitive LdAPx overexpression strain reduces DNA fragmentation compared to that of the sensitive wild-type strain (Fig. 8, lane 5). Positive-control, apoptotic (U937) cells show clear 180- to 200-bp nucleosomal fragments (Fig. 8, lane 6).

Reversion of the AmB resistance property by inhibitors. Aminotriazole, an inhibitor of APx, had no toxic effect on the untreated sensitive and resistant parasites. Preincubation with aminotriazole demonstrated partial reversion of the resistant property, as the LD$_{50}$ of AmB for the resistant strain decreased ~1.9-fold (Table 1). However, the LD$_{50}$ of the sensitive strain was

not altered by preincubation with aminotriazole (the LD$_{50}$ decreased ~1.01-fold). It has also been demonstrated that after preincubation of the sensitive LdAPx overexpression strain with aminotriazole, the LD$_{50}$ of AmB decreased to ~1.7-fold compared to that without treatment. These result clearly suggested that LdAPx has an important role in the ROS-scavenging mechanism.

DISCUSSION

Ascorbate peroxidase has been demonstrated in *Leishmania* to be required for detoxifying peroxidase activity (14). It is an extremely rare sugar, which is known only in polysaccharides of plants, not in polysaccharides of humans (13). In parasites, it plays a vital role in protecting against oxidative damage. The absence of this redox pathway in the human host may be exploited for therapeutic reasons. We report for the first time the presence of APx in *L. donovani* and an attempt to clone its sequence and understand the function of overexpressed LdAPx in AmB-resistant clinical isolates. It was observed that the AmB-resistant strain protects against AmB-induced apoptosis-like cell death by overexpressing

FIG 8 (A) Detection of protease activity in DNA. Shown is an overlay of the fluorescence histograms obtained for sensitive cells (green), sensitive cells in which LdAPx is overexpressed (black), and sensitive wild-type cells (red). (B) Comparison of TUNEL results for detecting apoptosis in sensitive and resistant promastigotes after AmB treatment. No positive cells were found in the control. (C) DNA fragmentation analysis by agarose gel electrophoresis. The DNA profiles for untreated or AmB-treated promastigotes and sensitive and resistant promastigotes preincubated with Z-VD-FMK after 24 h of incubation at 26°C are shown. Positive control, apoptotic U937 cells supplied by the manufacturer (Roche). Lane 1, markers; lane 2, DNA of the resistant strain preinhibited with aminotriazole; lane 3, DNA of sensitive overexpression strain after being preincubated with aminotriazole; lane 4, DNA from the sensitive AmB-treated strain; lane 5, DNA from the sensitive AmB-treated overexpression strain; lane 6, positive control; lanes 7 and 8, controls for sensitive and resistant strains, respectively.

LdAPx. The protective function of LdAPx is mediated by detoxification of an excess ROS burden, which prevents the loss of mitochondrial potential from a low level of cytosolic calcium. This results in a smaller release of reduced Cyt *c* (by upregulation of ascorbate as well as the trypanothione cascade) from mitochon-
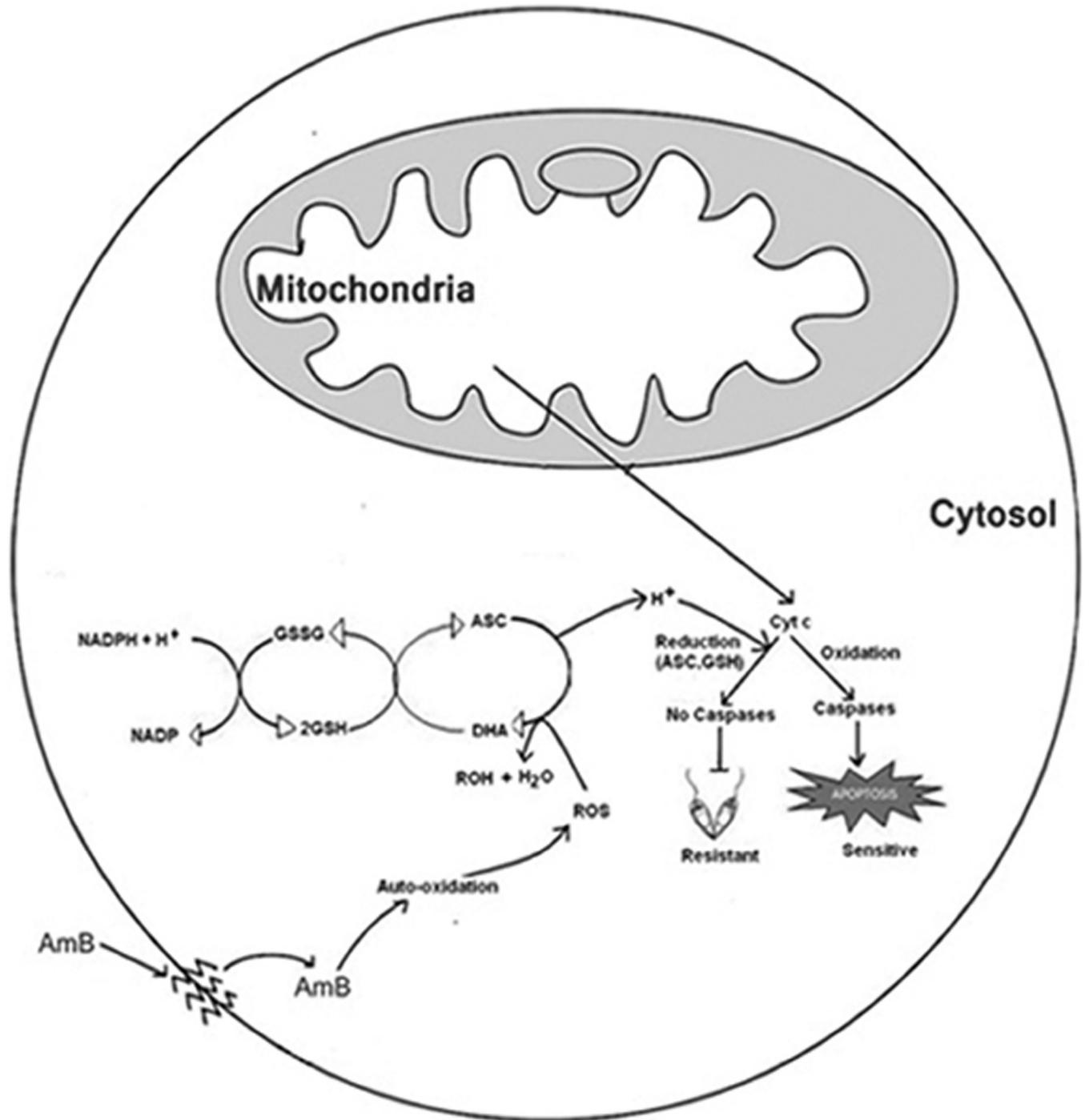
TABLE 1 Analysis of the partial reversion of the phenotype of the AmB-resistant strain using an ascorbate peroxidase inhibitor

Exptl set	LD$_{50}$ (μg/ml)[a]	Fold decrease from value for strain without aminotriazole
Resistant strain + AmB	0.837	
Sensitive strain + AmB	0.125	
Sensitive overexpression strain + AmB	0.631	
Resistant strain + AmB + aminotriazole	0.43	~1.9
Sensitive strain + AmB + aminotriazole	0.124	~1.02
Sensitive overexpression strain + AmB + aminotriazole	0.37	~1.70

[a] The LD$_{50}$s of AmB in the presence and absence of different inhibitors were calculated from *in vitro* drug sensitivity assays as described in Materials and Methods.

dria into the cytosol, which does not activate the caspase-like protease activity; therefore, AmB-resistant cells survive.

The *in silico* and *in vitro* ascorbate peroxidase inhibitory analysis shows that aminotriazole or sodium azide may be a good inhibitor. The interaction between the *L. donovani* APx binding site and 1H-1,2,4-triazol-5-amine (aminotriazole) suggests that the Glu133, Val 127, and Ser301 amino acids may play a key role in the inhibition of *L. donovani* APx (Fig. 3). The results of Adak and Datta (13), where they show that the removal of H$_2$O$_2$ by amastigotes was markedly inhibited by aminotriazole or sodium azide (an inhibitor of heme-containing enzymes), also support our data (13).

Lamy-Freund et al. reported that AmB may affect cells by generating free radicals after auto-oxidation (6). Reactive oxygen species (ROS) have been shown to be toxic but also function as signaling molecules. The pathways that regulate ROS homeostasis are crucial for mitigating the toxicity of ROS and provide strong evidence about specificity in ROS signaling. In the present study, we investigated the intracellular ROS level for both resistant and sensitive promastigotes after AmB treatment to predict whether or not ROS are the key molecules for AmB-mediated cell death. Several signal circuitries regulate protective responses to ROS-induc-

FIG 9 Hypothetical model showing intracellular events in conferring amphotericin B resistance. The model diagram illustrates that AmB inside the cells after auto-oxidation generates free radicals, which changes the mitochondrial membrane potential. Due to depolarization of the mitochondrial membrane, there is a release of Cyt *c* into the cytosol. The released cytochrome *c* is oxidized and moves toward apoptosis by means of caspase-like activity in the case of the sensitive strain but by means of the upregulation of ascorbate peroxidase in the case of the resistant strain, which is scavenged by the ascorbate-glutathione cascade, as is the by-product. ASC, ascorbate; DHA, dehydroascorbate; GSH, reduced glutathione; GSSG, oxidized glutathione. Ascorbate and glutathione also reduced the cytochrome *c* and bypassed the pathway of apoptosis.

ible oxidative stress or trigger apoptosis as a clearance mechanism for oxidatively damaged cells. Moreover, in our study, we observed that pretreatment of the resistant strain with aminotriazole (33) resulted in higher ROS production than in the sensitive wild-type strain but that the sensitive strain in which LdAPx was over-expressed had lower ROS production (Fig. 5), which suggests that resistant parasites use this enzyme to overcome oxidative stress.

The assessment of early mitochondrial alterations allows for the identification of cells that are committed to die but have not yet displayed the apoptosis-like phenotype. In our study, we ob-

served that the resistant strain had lower depolarization in its mitochondrial membrane than the sensitive strain, probably due to upregulation of LdAPx and the thiol metabolic-pathway genes (4) in the resistant strain, which may detoxify ROS activity (Fig. 6A and B). When we inhibited LdAPx with aminotriazole, the reversion of the resistant strain's property was observed (Fig. 6). We also observed that the sensitive LdAPx overexpression strain had reduced mitochondrial membrane potential compared to that of the sensitive wild-type strain. It shows that AmB-induced ROS has a probable role in the depolarization of mitochondrial membranes and that overexpressed LdAPx plays an important role in regulating the ROS-mediated mitochondrial membrane depolarization in the resistant strain (Fig. 6). In addition, the alteration in the Ca^{2+} level in the cytosol in response to ROS generation was also found to induce mitochondrial dysfunction. Inhibitors of ascorbate peroxidase prevented a substantial loss of mitochondrial potential and also significantly lowered the percentage of TUNEL-positive cells (Fig. 9).

It is well established that disruption of the outer mitochondrial membrane by apoptotic stimuli results in the release of cytochrome *c* into the cytoplasm, which activates a cascade of caspase-like proteases involved in apoptosis. In our study, we observed the release of cytochrome *c* directly proportional to ROS inside the cells (Fig. 7A). Furthermore, our study illustrates for the first time a relationship between the rate of Cyt *c* reduction by thiols and the activation of caspase-like protein. The present kinetics study offers insights into the potential role of thiols and ascorbate in regulating the cellular redox equilibrium of Cyt *c*, which may be implicated in the apoptosis process mediated by Cyt *c*. The activation of caspase-like protease is mediated, at least partly, by the release of cytochrome *c* from mitochondria into the cytosol. This process is sensitive to oxidative stress and endogenous reducing factors, including ascorbate, that are required for caspase activity to induce apoptosis.

The biochemical pathways that mediate apoptosis-like death in kinetoplastids are still unknown. In metazoans, release of cytochrome *c* into the cytosol leads to consequent activation of caspases, the principal effector molecules of apoptosis (41, 42). In *Leishmania*, the presence and role of caspases in apoptosis remain controversial, as Zangger et al. reported that stress-promoted death is caspase independent (43), whereas several other groups have also demonstrated caspase-dependent death (19, 41, 44). There is evidence that the caspase-like proteases play important roles in the apoptotic cascade of unicellular kinetoplastid parasites after induction of different stimuli (11, 44). The activation of the CED3/CPP32 group of proteases is well established in leishmanial cells (35, 36). Therefore, the possibility of the presence of caspase-like proteases in leishmanial cells cannot be ruled out. In the present study, we observed caspase-like proteases as well as metacaspase activity in leishmanial cells, both of which were found to be higher in the sensitive strain than in the resistant strain (Fig. 7D). Our data support the result of Zalila et al. (45), who showed that metacaspase overexpression enhanced *L. major* sensitivity to oxidative stress, as measured by the rapid loss of mitochondrial membrane potential, and suggest a role in *Leishmania* apoptosis. In the presence of the caspase 3 group of protease inhibitors (Z-VAD-FMK) or a metacaspase inhibitor (antipain), downstream events of caspase 3-like protease activation and metacaspase activation, such as DNA fragmentation, were prevented in the sensitive strains, which suggests that the proteases are involved in AmB-induced programmed cell death of leishmanial cells

(Fig. 8C). In our study, the release of cytochrome *c* was accompanied by the activation of CED3/CPP32 DEVDase activity, and its specificity was further substantiated by its reduction after treatment with DEVD-FMK, a CED3/CPP32-specific inhibitor. These results suggest that nuclear events are under the control of proteases sensitive to caspase inhibitors.

To investigate whether overexpression of LdAPx in the resistant strain shielded cells against oxidative-stress-mediated apoptosis, nuclear DNA fragmentation as a marker of apoptosis was measured. The sensitive AmB-treated strain led to a gradual conversion of viable cells into apoptotic cells that was greater than in the LdAPx-overexpressing resistant strain (Fig. 8A and B). Overexpression of LdAPx causes a decrease in the ROS burden, which is an early and critical event in preventing the release of Ca^{2+} ions, the loss of mitochondrial potential, and cytochrome *c* release from mitochondria to the cytosol, which suggests an increase in tolerance to H_2O_2 and protection against AmB-induced oxidative stress. The DNA fragmentation assay was assessed by the TUNEL assay, the results of which also support the above data (Fig. 8C).

The removal of H_2O_2 by amastigotes was markedly inhibited by aminotriazole or sodium azide, which is an inhibitor of heme-containing enzymes, e.g., catalase or peroxide (9). We also demonstrated the effect of an LdAPx pathway inhibitor on the resistant strain to find out whether both the glutathione-ascorbate pathway and the ABC transporter (overexpressed in the microarray) inhibitor have an effect on the partial reversion of the resistant strain. We also found that coinhibition has a more potent effect than inhibition by either the ABC transporter inhibitor or ascorbate peroxidase in reversing the resistant property of the resistant strain, as demonstrated by ~2.1-fold and ~1.9-fold changes with the ascorbate peroxidase pathway and ABC transporter inhibitors, respectively (Table 1). This probably indicates a synergistic involvement of both drug efflux and ROS-scavenging machinery in conferring AmB resistance.

Taken together, the data presented in this study identify protease activity (possibly caspase-like) as an important instigator and regulatory molecule in the cell death cascade in *L. donovani* when challenged by amphotericin B (Fig. 9). Amphotericin B-induced alteration in membrane permeability, including in mitochondria, leads to the release of cytochrome *c* from the mitochondria to the cytosol, thus activating proteases (metacaspase- and caspase-like proteins). As a result, it activates DNase, which causes nuclear DNA fragmentation, resulting in apoptosis-like cell death. Although the current study was conducted with drug-resistant promastigotes, the leads obtained will certainly be valuable in understanding the modes of actions of drugs.

REFERENCES

1. **World Health Organization.** 1998. The world health report. Life in the 21st century. A vision for all. World Health Organization, Geneva, Switzerland.
2. **Chappuis F, Sundar S, Hailu A, Ghalib H, Rijal S, Peeling RW, Alvar J, Boelaert M.** 2007. Visceral leishmaniasis: what are the needs for diagnosis, treatment and control. Nat. Rev. Microbiol. **5:**873–882. http://dx.doi.org/10.1038/nrmicro1748.
3. **Pinto da Costa Tavares JA, Ouaissi A, Cordeiro-da-Silva A.** 2008.

Therapy and further development of anti-leishmanial drugs. Curr. Drug Ther. **3**:204–208. http://dx.doi.org/10.2174/157488508785747871.

4. **Purkait B, Kumar A, Nandi N, Sardar AH, Das S, Kumar S, Pandey K, Ravidas V, Kumar M, De T, Singh D, Das P.** 2012. Mechanism of amphotericin B resistance in clinical isolates of *Leishmania donovani*. Antimicrob. Agents Chemother. **56**:1031. http://dx.doi.org/10.1128/AAC.00030-11.

5. **Mbongo N, Loiseau PM, Billion MA, Robert-Gero M.** 1998. Mechanism of amphotericin B resistance in *Leishmania donovani* promastigotes. Antimicrob. Agents Chemother. **42**:352–357.

6. **Lamy-Freund MT, Ferreira VFN, Schreier S.** 1985. Mechanism of inactivation of the polyene antibiotic amphotericin B: evidence for radical formation in the process of autooxidation. J. Antibiot. **38**:753–757. http://dx.doi.org/10.7164/antibiotics.38.753.

7. **Boveris A, Sies H, Martino EE, Docampo R, Turrens JF, Stoppani AO.** 1980. Deficient metabolic utilization of hydrogen peroxide in *Trypanosoma cruzi*. Biochem. J. **188**:643–648.

8. **Fairlamb AH, Cerami A.** 1992. Metabolism and functions of Trypanothione in the Kinetoplastida. Annu. Rev. Microbiol. **46**:695–729. http://dx.doi.org/10.1146/annurev.mi.46.100192.003403.

9. **McGonigle S, Dalton JP, James ER.** 1998. Peroxidoxins: a new antioxidant family. Parasitology **14**:139–145.

10. **Nogoceke E, Gommel DU, Kiess M, Kalisz HM, Flohe L.** 1997. A unique cascade of oxidoreductases catalyses trypanothione mediated peroxide metabolism in *Crithidia fasciculate*. Biol. Chem. **378**:827–836.

11. **Wilkinson SR, Obado SO, Mauricio IL, Kelly JM.** 2002. *Trypanosoma cruzi* expresses a plant-like ascorbate dependent hemoperoxidase localized to the endoplasmic reticulum. Proc. Natl. Acad. Sci. U. S. A. **99**:13453–13458. http://dx.doi.org/10.1073/pnas.202422899.

12. **Meister A.** 1994. Glutathione, ascorbate, and cellular protection. Cancer Res. **54**(7 Suppl):1969s–1975s.

13. **Adak S, Datta AK.** 2005. *Leishmania major* encodes an unusual peroxidase that is a close homologue of plant ascorbate peroxidase: a novel role of the transmembrane domain. Biochem. J. **390**:465–474. http://dx.doi.org/10.1042/BJ20050311.

14. **Dolai S, Yadav RK, Pal S, Adak S.** 2008. Leishmania major ascorbate peroxidase overexpression protects cells against reactive oxygen species-mediated cardiolipin oxidation. Free Radic. Biol. Med. **45**:1520–1529. http://dx.doi.org/10.1016/j.freeradbiomed.2008.08.029.

15. **Phillips AJ, Sudbery I, Ramsdale M.** 2003. Apoptosis induced by environmental stresses and amphotericin B in *Candida albicans*. Proc. Natl. Acad. Sci. U. S. A. **100**:14327–14332. http://dx.doi.org/10.1073/pnas.2332326100.

16. **Mousavi SA, Robson GD.** 2004. Oxidative and amphotericin B-mediated cell death in the opportunistic pathogen *Aspergillus fumigatus* is associated with an apoptotic-like phenotype. Microbiology **150**:1937–1945. http://dx.doi.org/10.1099/mic.0.26830-0.

17. **Smirlis D, Duszenko M, Ruiz AJ, Scoulica E, Bastien P, Fasel N, Soteriadou K.** 2010. Targeting essential pathways in trypanosomatids gives insights into protozoan mechanisms of cell death. Parasit. Vectors **3**:107. http://dx.doi.org/10.1186/1756-3305-3-107.

18. **Jiang X, Wang X.** 2004. Cytochrome c mediated apoptosis. Annu. Rev. Biochem. **73**:87–106. http://dx.doi.org/10.1146/annurev.biochem.73.011303.073706.

19. **Ludovico P, Rodrigues F, Almeida A, Silva MT, Barrientos A, CorteReal M.** 2002. Cytochrome c release and mitochondria involvement in programmed cell death induced by acetic acid in *Saccharomyces cerevisiae*. Mol. Biol. Cell **13**:2598–2606. http://dx.doi.org/10.1091/mbc.E01-12-0161.

20. **Butler J, Koppenol WH, Margoliash E.** 1982. Kinetics and mechanism of the reduction of ferricytochrome c by the superoxide anion. J. Biol. Chem. **257**:10747–10750.

21. **Goldkorn T, Schejter A.** 1979. Electrostatic effects on the kinetics of oxidation-reduction reactions of c-type cytochromes. J. Biol. Chem. **254**:12562–12566.

22. **Myer YP, Kumar S.** 1984. Ascorbate reduction of horse heart cytochrome c. A zero-energy reduction reaction. J. Biol. Chem. **259**:8144–8150.

23. **Al-Ayash AI, Wilson MT.** 1979. The mechanism of reduction of single-site redox proteins by ascorbic acid. Biochem. J. **177**:641–648.

24. **Williams NH, Yandell JK.** 1985. Reduction of oxidized cytochrome c by ascorbate ion. Biochim. Biophys. Acta **810**:274–277. http://dx.doi.org/10.1016/0005-2728(85)90142-2.

25. **Kujundzic N, Everse J.** 1978. Reduction of horse heart ferricytochrome c by glutathione: evidence for two different conformational forms of ferricytochrome c in neutral and slightly alkaline solutions. Biochem. Biophys. Res. Commun. **82**:1211–1216. http://dx.doi.org/10.1016/0006-291X(78)90316-9.

26. **Subudhi U, Chainy GB, Mohanty P.** 2006. Kinetics and mechanism of reduction of ferricytochrome c by glutathione and L-cysteine: a comparative study. Indian J. Biochem. Biophys. **43**:37–40.

27. **Hu T-M, Ho S-C.** 2011. Kinetics of redox interaction between cytochrome c and thiols. J. Med. Sci. **31**(3):109–115.

28. **Debnath A, Sen A, Mckerrow JH, Das P.** 2004. Role of DNA microarray technology for understanding differential gene expression in parasitic diseases. J. Parasit. Dis. **28**:5–16.

29. **Sali B.** 1993. Comparative protein modelling by satisfaction of spatial restraints. J. Mol. Biol. **234**(3):779–815. http://dx.doi.org/10.1006/jmbi.1993.1626.

30. **Ruben L, Hutchinson A, Moehlman J.** 1991. Calcium homeostasis in *Trypanosoma brucei*. J. Biol. Chem. **266**:24351–24358.

31. **Singh G, Jayanarayan KG, Dey CS.** 2005. Novobiocin induces apoptosis-like cell death in topoisomerase II over-expressing arsenite resistant *Leishmania donovani*. Mol. Biochem. Parasitol. **141**:57–69. http://dx.doi.org/10.1016/j.molbiopara.2005.01.014.

32. **Lee N, Bertholet S, Debrabant A, Muller J, Duncan R, Nakhasi HL.** 2002. Programmed cell death in the unicellular protozoan parasite Leishmania. Cell Death Differ. **9**:53–64. http://dx.doi.org/10.1038/sj.cdd.4400952.

33. **Suto D, Kazuaki S, Yoshiro O, Yoshimura T, Fujii J.** 2005. Suppression of pro-apoptotic function of cytochrome c by singlet oxygen via a heme redox state-independent mechanism. Biochem. J. **392**:399–406. http://dx.doi.org/10.1042/BJ20050580.

34. **Mukherjee SB, Das M, Sudhandiran G, Shaha C.** 2002. Increase in cytosolic $Ca+2$ levels through the activation of non selective cation channels induced by oxidative stress causes mitochondrial depolarization leading to apoptosis-like death in *L. donovani* promastigotes. J. Biol. Chem. **277**:24717–24727. http://dx.doi.org/10.1074/jbc.M201961200.

35. **Sen N, Das BB, Ganguly A, Mukherjee T, Bandyopadhyay S, Majumder HK.** 2004. Camptothecin-induced imbalance in intracellular cation homeostasis regulates programmed cell death in unicellular hemoflagellate *Leishmania donovani*. J. Biol. Chem. **279**:52366–52375. http://dx.doi.org/10.1074/jbc.M406705200.

36. **Sen N, Das BB, Ganguly A, Mukherjee T, Tripathi G, Bandyopadhyay S, Rakshit S, Sen T, Majumder HK.** 2004. Camptothecin induced mitochondrial dysfunction leading to programmed cell death in unicellular hemoflagellate *Leishmania donovani*. Cell Death Differ. **11**:924–936. http://dx.doi.org/10.1038/sj.cdd.4401435.

37. **Brown GC, Borutaite V.** 2008. Regulation of apoptosis by the redox state of cytochrome c. Biochim. Biophys. Acta **1777**:877–881. http://dx.doi.org/10.1016/j.bbabio.2008.03.024.

38. **Kupchan SM, Anderson WK, Bollinger P, Doskotch RW, Smith RM, Renauld JA, Schnoes HK, Burlingame AL, Smith DH.** 1969. Tumor inhibitors. XXXIX. Active principles of *Acnistus arborescens*. Isolation and structural and spectral studies of withaferin A and withacnistin. J. Org. Chem. **34**:3058–3866.

39. **Zou H, Henzel WJ, Liu X, Lutschg A, Wang X.** 1997. Apaf-1, a human protein homologous to C. elegans CED-4, participates in cytochrome c-dependent activation of caspase-3. Cell **90**:405–413. http://dx.doi.org/10.1016/S0092-8674(00)80501-2.

40. **Wyllie AH.** 1980. Glucocorticoid-induced thymocyte apoptosis is associated with endogenous endonuclease activation. Nature **284**:555–556. http://dx.doi.org/10.1038/284555a0.

41. **Debrabant A, Lee N, Bertholet S, Duncan R, Nakhasi HL.** 2003. Programmed cell death in trypanosomatids and other unicellular organisms. Int. J. Parasitol. **33**:257–267. http://dx.doi.org/10.1016/S0020-7519(03)00008-0.

42. **Nagata S.** 2000. Apoptotic DNA fragmentation. Exp. Cell Res. **256**:12–18. http://dx.doi.org/10.1006/excr.2000.4834.

43. **Zangger H, Mottram JC, Fasel N.** 2002. Cell death in *Leishmania* induced by stress and differentiation: programmed cell death or necrosis? Cell Death Differ. **9**:1126–1139. http://dx.doi.org/10.1038/sj.cdd.4401071.

44. **Das M, Mukherjee SB, Shaha C.** 2001. Hydrogen peroxide induces apoptosis-like death in *Leishmania donovani* promastigotes. J. Cell Sci. **114**:2461–2469.

45. **Zalila H, Gonzalez IJ, El-Fadili AK, Delgado MB, Desponds C, Schaff C, Fasel N.** 2011. Processing of metacaspase into a cytoplasmic catalytic domain mediating cell death in *Leishmania major*. Mol. Microbiol. **79**:222–239.